IEEE Transactions on Nuclear Science, Vol.NS-24, No.3, June 1977

COLLECTIVE ION ACCELERATION AND POWER BALANCE IN INTENSE ELECTRON BEAMS IN NEUTRAL GAS*

B. Ecker and S. Putnam
Physics International Company
2700 Merced Street
San Leandro, CA 94577

The documented collective acceleration of background gas ions by intense electron beams has achieved proton-to-electron energy ratios above 15,[1] corresponding to 14 MeV protons, and is characterized by equal ion and beam front velocities.[2,3] In order to guide experiments aimed at scaling to higher particle energies, it has been important to adequately understand the physics controlling the beam front velocity, $\beta_f c$, which is experimentally found to be considerably less than the injected electron velocity. We present new proton collective acceleration data that disagree with the space-charge-limited β_f models,[4,5] but are in accord with a power balance β_f model that emphasizes the beam electron energy losses connected with self-magnetic field generation. Independent measurements are also presented that qualitatively confirm the predicted electron energy loss and its variation with experimental parameters.

INTRODUCTION

In 1968 it was discovered[6] that an intense electron beam propagating through initially neutral low-pressure gas can collectively accelerate a compact bunch of background gas ions. One of the more important findings to come out of the early studies[2,3] of this CA mode in hydrogen was the matching of the final proton velocity, $\beta_p c$, and the beam front velocity, $\beta_f c$, in the acceleration region (the first ~ 20 cm of beam propagation):

$$\beta_p c = \beta_f c \tag{1}$$

Together with additional data showing a spatial association of the accelerated proton bunch and the beam front, Eq. (1) has formed the empirical basis for the now widely held view that the "zero-order" electrostatic potential well of the non-charge-neutralized beam front is responsible for the observed trapping and acceleration of background gas ions. Accelerating fields of order 1 MV/cm are implied by the data.[3]

In general, the advancing head or front of an intense electron beam in neutral gas constitutes a net negative charge cloud which is replenished from behind. The beam is fully charge-neutralized behind the front (by definition) as a result of gas ionization and secondary electron expulsion. The relation $\beta_p = \beta_f$ has motivated our studies to focus on identifying the physics governing β_f. The data thus gathered was found to have serious inconsistencies with the Olson β_f model.[5] The problem was found to be the neglect of important beam energy dissipation effects connected with beam self-fields. To account for these effects, we have invoked and extended the beam power balance analysis used previously by Graybill et al.,[7] which does not really pertain explicitly to collective acceleration (CA) at all, but to an energy conservation constraint on intense electron beam front propagation velocity, $\beta_f c$. The power balance model for β_f is then straightforwardly linked to collective acceleration by Eq. (1). We proceed now to describe the power balance picture in relation to the phenomenology introduced by Rostoker[4] and re-explored by Olson.[5]

BEAM FRONT PROPAGATION IN LOW-PRESSURE NEUTRAL GAS

As indicated by Rostoker,[4] the phenomenological form of the physics controlling β_f is simply

$$\beta_f = \frac{\mathcal{L}}{c\,\tau_N(p)} \tag{2}$$

where $\mathcal{L}$ is the length of the beam front, i.e., the non-charge-neutral leading portion of the beam in which gas ionization leading to charge neutralization is occurring, and τ_N is the charge neutralization time, i.e., the time required for gas ionization to charge-neutralize the beam to the level permitting complete propagation. τ_N depends on the gas pressure, p, and type. Equation (2) says that the beam front can advance only so fast as is permitted by the process of charge neutralization via gas ionization. Equation (2) was used by Rostoker[4] and again by Olson[5] with different calculations for $\mathcal{L}$ and τ_N. It is important to note that the form of Eq. (2) stands by itself, independent of specific models for $\mathcal{L}$ and τ_N. In both the Rostoker and Olson treatments, $\mathcal{L}$ was assumed to be governed by purely electrostatic forces arising from the unneutralized space charge of the beam front. However, our experimental data on β_f cannot be explained even qualitatively unless the electron energy losses associated with self-field generation are taken into account. Figure 1 shows data from the case with 0.55 torr hydrogen in the acceleration chamber. In the figure, β_p and β_f are jointly signified by the symbol $\beta_{f,p}$, and $\mathcal{E}_p$ is the proton kinetic energy. It is seen that β_f is an increasing function of $Z \equiv \mathcal{E}_e/I_o e$, the diode impedance or beam electron energy-to-current ratio at injection, and of the injected beam radius r_b, which was varied by changing the cathode radius, r_c. While neither of these β_f effects are predicted by the Olson model (which gives the dashed line in the figure), they can be understood in terms of beam kinetic energy loss due to self-magnetic field generation, as we now show.

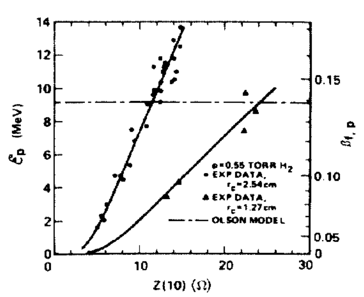

Figure 1 $\mathcal{E}_p$ and $\beta_{f,p}$ versus Z for two cathodes of different radius, at 0.55 torr H_2.

The direct calculation of $\mathcal{L}$, which is needed in Eq. (2), is analytically intractable, so we instead use a power balance analysis to bring out the physics. To illustrate the power balance most simply, we first consider the limiting case in which self-magnetic field generation consumes all of the injected electron energy:

$$P_o = P_M \tag{3}$$

where $P_o = (1/e)\,\mathcal{E}_e I_o$ is the injected beam power and P_M is the rate of energy flow into the self-magnetic field, given by the product of the beam front velocity and the magnetic field energy per unit length, hence

$$P_M = \frac{\mu_o c}{16\pi}\left(1 + 4\,\ln\frac{r_w}{r_b}\right) I_o^{\,2}\,\beta_f \qquad (4)$$

Here it has been assumed that the axial beam current density is uniform, that there is no current neutralization (which is experimentally the case in the gas pressure range supporting this CA mode), and that the beam chamber is a conducting cylinder of wall radius r_w. Equation (3) is solved for β_f to give

$$\beta_f = \frac{16\pi}{\mu_o c}\,\frac{Z}{1 + 4\,\ln\dfrac{r_w}{r_b}} \qquad (5)$$

The data (Fig. 1) and Eq. (5) clearly agree regarding the manner in which Z and r_b affect $\beta_{f,p}$. We emphasize that Eq. (5) represents the special limiting condition, Eq. (3), and so only serves in the present context to bring out the qualitative physics associated with the self-magnetic field effect.

From the point of view of Eq. (2), the generation of the azimuthal self-magnetic field involves an induced axial electric field which decelerates electrons, making $\mathcal{L}$ smaller than in the purely charge-limited case. When Z or r_b is increased, the effect of the induced electric field decreases, either relatively or absolutely, allowing $\mathcal{L}$ to grow larger and β_f to increase. The fact that the scaling of β_f seems dominated by magnetic energy production (as epitomized by Eq. (3)) means that the induced electric field plays a role which is at least as important as that of the electrostatic field in determining $\mathcal{L}$, and perhaps much more so.

DETECTION OF ELECTRON ENERGY LOSSES

The view that β_f is controlled by power balance effects involving major electron energy losses gets strong support from time-resolved measurements of bremsstrahlung X-rays generated by electrons striking chamber walls. A representative waveform is shown in Fig. 2 (0.55 torr case). A fast scintillator-photodiode combination was used to monitor the X-ray intensity, which was relatively low during the initial phase when the beam front was moving toward the chamber endplate, with the electrons striking the sidewall. In this phase the electrons flow through the beam front to the sidewall; it is in the beam front that self-field generation would extract energy. Just when the beam front reached the endplate and effectively disappeared into it (82 cm from the beam injection window), the X-ray intensity increased dramatically and abruptly, indicating a significant increase in the energy with which the electrons hit the wall. This energy increase occurred because the electrons now struck the endplate without having to traverse a lossy front region. In a purely electrostatic system, electrons would always have full energy upon reaching any wall (so long as the chamber is a grounded conductor, as in our case). There were no fluctuations in injected electron energy or current that could account for the observed change of X-ray intensity. The correspondence of the X-ray burst with the beam front's arrival at the endplate was confirmed by Rogowski coil measurements of beam front position vs. time.

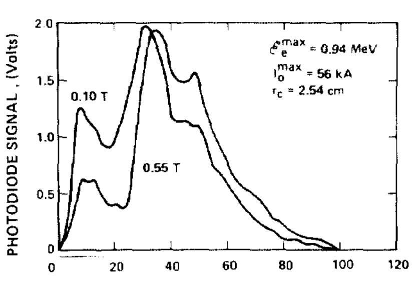

Figure 2 Representative X-ray bremsstrahlung waveforms at two gas pressures, showing (in 0.55 torr case) an initial low-amplitude phase due to electron energy losses in beam front.

GAS PRESSURE EFFECT IN POWER BALANCE PICTURE

Equations (3) to (5) bring out the role of beam and geometry parameters in the power balance control of $\beta_{f,p}$, but do not yet contain the gas density or pressure, p, that has been shown[8] to strongly influence $\beta_{f,p}$. Figure 3 presents additional hydrogen pressure variation data for five different beams.

Note in Fig. 3 that $\beta_{f,p}$ varies with beam parameters at all pressures. According to the Olson model,[5] $\beta_{f,p}$ should be independent of beam parameters (except in the relatively uninteresting low-pressure range, below about 0.2 torr here), and β_f should begin to depend on beam parameters via power balance only as p exceeds the high-pressure cut-off of collective acceleration.

From Fig. 3 it is seen that β_p and $\beta_{f,p}$ increase with p (except for certain exceptions which are discussed later). This behavior follows directly from Eq. (2), since τ_N should decrease when p increases. But as already shown, without a realistically complete calculation of $\mathcal{L}$, Eq. (2) does not bring out the dominant physics, and so we turned to the power balance analysis. To complete that picture, we now describe the role of the gas pressure in it.

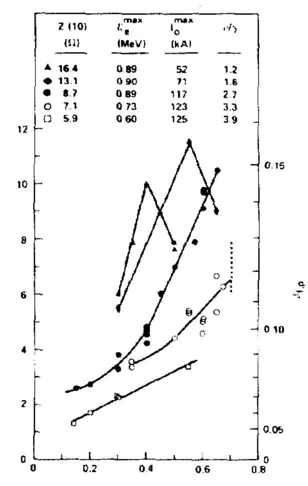

Figure 3 $\mathcal{E}_p$ and $\beta_{f,p}$ vs H_2 pressure (5 beams).

Equation (5) is unphysical regarding the pressure because it contains only one quantity, β_f, that should vary with pressure (via τ_N in Eq. (2)). This incompleteness is due to having taken the limiting case [Eq. (3)] in which all the injected kinetic energy goes into self-magnetic field energy. But as documented by the X-ray data, there is a residual electron kinetic energy that strikes the chamber wall, producing X-rays. The missing term in Eq. (3) is just the kinetic power flow into the wall, P_W:

$$P_o = P_M + P_W \qquad (6)$$

Equation (6), together with Eq. (4), simply says that when β_f increases due to increased pressure, P_M is increased, i.e., self-field generation consumes a greater portion of electron energy, so electron energy at wall impact is reduced. Therefore P_W decreases, with a corresponding decrease of X-ray intensity during the lossy period before the beam front reaches the endplate. Figure 2 shows that the X-ray waveforms indeed exhibit this behavior, verifying that at fixed beam parameters, an increased beam front velocity causes increased non-conservative electron energy losses, in accordance with power balance.

Returning, as promised, to the down-turn of some of the curves in Fig. 3, we note that the collective acceleration is impaired if Z and/or p is too high, presumably because β_f is then too high for proton trapping to occur; the protons slip behind the moving potential well either immediately (resulting in no detected protons) or after gaining only some portion of the energy which they would have had if $\beta_p = \beta_f$, so that actually $\beta_p < \beta_f$. This would be the reason for the down-turn in some of the curves in Fig. 3. The obvious solution to this limitation is to have Z and p smoothly increase during acceleration from relatively low values (Z in time, p in space), so that β_f likewise increases from a low value. In this way the beam front could trap the protons at a suitably low velocity and then make a smooth transition (preserving trapping) to velocities above the present limits set by trapping kinematics.

The increase of Z (the diode impedance) in time is opposite the usual behavior of conventional intense beam diodes, but might be suitably achieved using a plasma-filled diode.[9] This diode technique is still in its infancy and is not really ready for this application. We therefore turn to the other option, consisting of a pressure gradient, with p increasing with propagation distance. From Fig 3 it is evident that considerable increases of $\mathcal{E}_p$ require only modest extensions to higher pressures using gradients. (Previous work[10] documented beam front velocity of 0.7 c in uniform 1 torr hydrogen, which is less than twice the present pressure cut-off; at 0.7 c, $\mathcal{E}_p$ would be 375 MeV.)

The pressure gradient technique has been attempted in two reported studies.[11,12] In both cases, serious flaws in the experiment account for the negative results obtained. In one case,[11] the increasing "gradient" was a single discontinuity of up to 0.85 torr at a distance of 30 cm from the anode. A thin conducting membrane was used to make the pressure differential. Recent experiments at PI have shown that abrupt pressure discontinuities completely disrupt the collective acceleration.

The other study[12] used smooth density gradients, but was seriously compromised by a rather slow beam current risetime of 70 nsec. Due to the slow risetime, the injected current, I_o, was below the space-charge-limiting current, I_ℓ, for about 40 nsec (according to the authors), as compared with about 1 nsec in our case. Since collective acceleration cannot occur until $I_o > I_\ell$,[5,13] their beam was streaming through and preionizing the gas for 40 nsec prior to acceleration onset. The effect of the gas density gradient cannot be evaluated in such a case. (Note that very low-level preionization was observed in another study[14] to quite strongly influence beam propagation in a manner that is not yet understood.)

CONCLUSION

The power balance physics governing $\beta_{f,p}$ has been described here as simply as possible, but detailed consideration reveals a very intricate web of self-consistent effects comprising the power balance picture. We have attempted to diagram the coupled physics logic in Fig. 4. The scenario shown in the figure integrally includes the electrostatic part of the problem emphasized by Olson.

(For completeness we mention that the localized pinch ["focusing instability"] mode[15,16] of collective acceleration should not be directly subject to the power balance constraint, since that mode does not depend on beam front velocity, provided that the beam front is sufficiently far ahead of the acceleration region.)

The problem of detailed, quantitative analysis of $\beta_{f,p}$ is one of non-laminar electron trajectory calculations, self-consistently coupled to strong electrodynamic and electrostatic self-fields and, equally important, to gas ionization processes (which have been theoretically evaluated by Olson,[17] but still await experimental documentation). The full intricacy of the problem can be gleaned through contemplation of Fig. 4. Fortunately, the semi-quantitative scaling laws represented by Eqs. (2) and (4)-(6) are quite enough to guide continuing experiments aimed at achieving interestingly high ion energies with this collective acceleration technique.

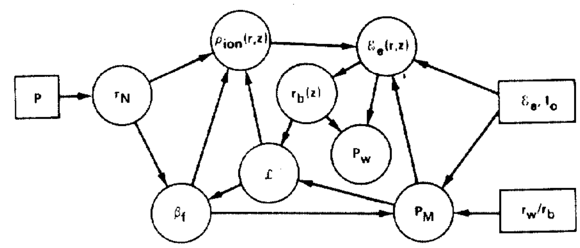

Figure 4 Causal relationships controlling intense electron beam front propagation in low-pressure neutral gas. Arrows extend from each quantity to those it directly influences; rectangles signify independent variables.

REFERENCES

*Work supported by USERDA

1. B. Ecker and S. Putnam, Proceedings of the Second Symposium on Collective Methods of Acceleration, JINR, DUBNA, USSR (1976); B. Ecker and S. Putnam, Bull. Am. Phys. Soc. 21, 1959 (1976).
2. J. Rander, Phys. Rev. Letters 25, 893 (1970).
3. B. Ecker and S. Putnam, IEEE Trans. Nucl. Sci. NS-20, 301 (1973).
4. N. Rostoker, Cornell University Laboratory of Plasma Studies, Report No. LPS 21 (July 1969).
5. C. L. Olson, Phys. Fluids 18, 585 (1975).
6. S. Graybill, et al., Ion Physics Corp. Rept. DASA 2315 (1968).
7. S. E. Graybill and J. R. Uglum, J. Appl. Phys. 41, 236 (1970).
8. D. Drickey, et al., Proc. 9th Interational Conf. on High Energy Accelerators, Stanford, CA ., May (1974)
9. P. Miller, J. Poukey, and T. Wright, Phys. Rev. Letters, 35, 940 (1975).
10. J. Rander, B. Ecker, G. Yonas, PIIR-9-70, Physics International Company, San Leandro, CA (1969).
11. A. A. Kolomensky, Proc. of the International Topical Conference on Electron Beam Research and Technology, Albuquerque, N.M., Nov. 1975, p. 295.
12. D. W. Swain, et al., Proc. 9th International Conference on High Energy Accelerators, SLAC, May (1974), p. 268.
13. D. C. Straw and R. B. Miller, Appl. Phys. Letters 25, 379 (1974).
14. D. Prono, et al., PIFR-557, Physics International Company, San Leandro, CA., February (1975).
15. S. Putnam, Phys. Rev. Letters 25, 1129 (1970).
16. K. V. Khodataev and V. N. Tsytovich, Sov. J. Plasma Phys. 2, 164 (1975). (Fiz. Plasmy 2, 301, 1976).
17. C. L. Olson, Phys. Rev. A 11, 288 (1975).